Letter to the Editor

Imaging findings in malignant hepatic infiltration from neuroendocrine tumor presenting with acute liver failure and mimicking cirrhosis: a case description

Marco Parillo[1,2]^, Federica Vaccarino[1,2], Chiara Taffon[1,3], Sara Vantaggi[1,3], Silvia Maria Rossi[1,3], Bruno Beomonte Zobel[1,2], Carlo Augusto Mallio[1,2]

[1]Fondazione Policlinico Universitario Campus Bio-Medico, Rome, Italy; [2]Research Unit of Diagnostic Imaging and Interventional Radiology, Department of Medicine and Surgery, Università Campus Bio-Medico di Roma, Rome, Italy; [3]Research Unit of Pathology, Department of Medicine and Surgery, Università Campus Bio-Medico di Roma, Rome, Italy

Correspondence to: Carlo Augusto Mallio, MD, PhD. Fondazione Policlinico Universitario Campus Bio-Medico, Via Alvaro del Portillo, 200, 00128 Rome, Italy; Research Unit of Diagnostic Imaging and Interventional Radiology, Department of Medicine and Surgery, Università Campus Bio-Medico di Roma, Rome, Italy. Email: c.mallio@policlinicocampus.it.

Submitted Jul 21, 2023. Accepted for publication Sep 28, 2023. Published online Oct 20, 2023.
doi: 10.21037/qims-23-1037
View this article at: https://dx.doi.org/10.21037/qims-23-1037

Introduction

Acute liver failure (ALF) is a critical condition with significant and sudden damage to the liver, encephalopathy, and impaired synthetic function lasting less than 26 weeks, occurring in individuals without cirrhosis or any preexisting liver ailments (1).

Diffuse hepatic infiltration by malignant cells can be a rare cause of ALF. In a study conducted in the United Kingdom, only 18 patients (0.45%) exhibited malignant liver infiltration out of 4,020 with ALF (2). In a more recent investigation carried out in the United States, a total of 27 cases (1.41%) of ALF resulting from malignant hepatic infiltration were observed out of 1,910 ALF cases; hematologic malignancies and breast cancer emerged as the primary causes, while a single patient exhibited ALF associated with small cell lung cancer (SCLC) (3). Neuroendocrine tumors (NETs) encompass a diverse array of tumors originating from neuroendocrine cells. While liver metastases are commonly seen in NET, the occurrence of malignant hepatic infiltration with a miliary pattern is a rarer finding, and the number of reported cases in the literature is limited (4-11).

In addition to its rarity, the diagnosis of malignant hepatic infiltration is challenging since it can clinically and radiologically mimic cirrhosis of the liver [so-called "pseudocirrhosis" (12)] with obvious implications for the patient's treatment course.

We present a case of pseudocirrhosis secondary to miliary liver metastases from a NET (possible SCLC) with complete image documentation in terms of pathology, ultrasound, computed tomography, and magnetic resonance imaging, also using a hepatobiliary contrast agent.

Case presentation

All procedures performed in this study were in accordance with the ethical standards of the institutional and/or national research committee(s) and with the Helsinki Declaration (as revised in 2013). Written informed consent was obtained from the patient for publication of this case report and accompanying images. A copy of the written consent is available for review by the editorial office of this journal.

We present the case of a 57-year-old man who was

^ ORCID: 0000-0002-4067-7118.

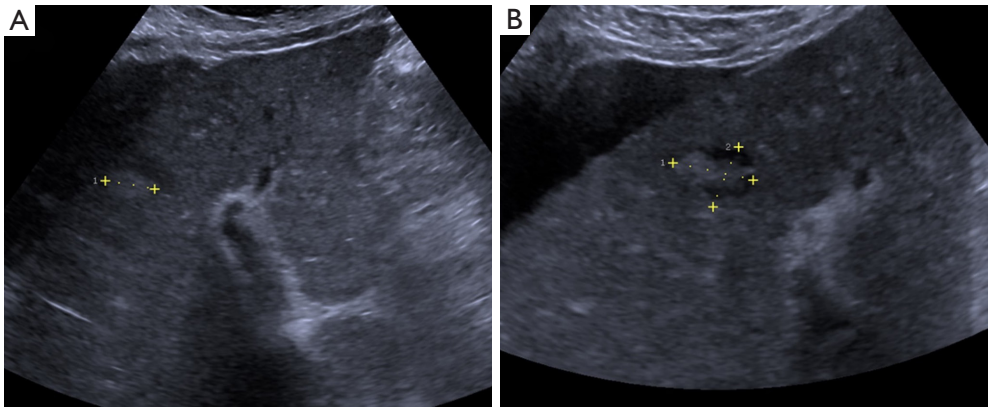

Figure 1 Ultrasound images of the right upper quadrant of the abdomen. (A,B) Liver ultrasound show an irregularly margined liver with multiple sub- and peri-centimetric hyperechoic nodules (calipers), accompanied by a significant amount of ascites.

admitted to the emergency department with jaundice and an incipient worsening of his general clinical condition, with cognitive-motor slowing. The patient exhibited a progressive increase in abdominal circumference and a weight gain of approximately 10 kg over the past 10 days, accompanied by fatigue and the subsequent development of hypochromic stools and dark urine.

He had a medical history of smoking, arterial hypertension, hyperlipidemia, insulin-dependent diabetes mellitus, and obesity, complicated by ischemic-hypertensive heart disease and peripheral arterial disease. No history of chronic liver diseases was reported.

Blood tests showed significant elevations in liver enzymes and cholestasis markers. The levels of total bilirubin were 23.7 mg/dL, of direct bilirubin were >15 mg/dL, of gamma-glutamyl transferase were 1,370 U/L, of alkaline phosphatase were 495 U/L, of aspartate aminotransferase (AST) were 135 U/L, and of alanine aminotransferase (ALT) were 94 U/L. Additionally, coagulation indices were impaired [prothrombin time: 27.3 seconds; international normalized ratio (INR): 2.1; activated partial thromboplastin time: 37.2 seconds].

Furthermore, an abdominal ultrasound examination (*Figure 1*) was performed, revealing a significant amount of ascitic fluid and a liver with polygonal and irregular margins, suggestive of chronic liver disease with cirrhotic features without dilatation of the bile ducts. Multiple liver nodules were also observed, resembling regeneration nodules.

The whole-body contrast-enhanced computed tomography (CT) scan (*Figure 2*) confirmed the presence of ascites and showed 2 hypervascular liver areas without definitive washout in the portal and delayed phases referable to transient hepatic attenuation differences; numerous, tiny, and widespread hypodense liver nodules were also observed. Chest CT scan documented a parenchymal consolidation located in the upper lobe of the right lung, associated with multiple mediastinal lymphadenopathies. Moreover, multiple bone lesions, suspicious for metastases, were identified.

The subsequent gadolinium ethoxybenzyl-diethylenetriamine pentaacetic acid (Gd-EOB-DTPA)-enhanced magnetic resonance imaging (MRI) examination (*Figure 3*) revealed several liver nodules and widespread hepatic restriction of proton diffusivity in diffusion weighted-imaging (DWI) images. No arterial phase hyperenhancement or non-peripheral washout suspected of hepatocellular carcinoma was reported. The hepatobiliary phase of the study cannot be evaluated due to the lack of Gd-EOB-DTPA uptake by the hepatic cells secondary to liver function impairment. In fact, there was no visible excretion of the contrast agent through the biliary system 20 minutes, as well as, 35 minutes after intravenous contrast agent administration.

The overall radiological picture was thus interpreted as suspicion for miliary liver metastases secondary to lung cancer, and the execution of a liver biopsy was recommended for histological confirmation.

The patient underwent a percutaneous biopsy of the liver parenchyma confirming the radiological hypothesis of disseminated hepatic metastases. In fact, the histological examination revealed a hepatic interstitial localization of malignancy, characterized by a variable growth pattern of solid cords and organoid nests of neoplastic neuroendocrine

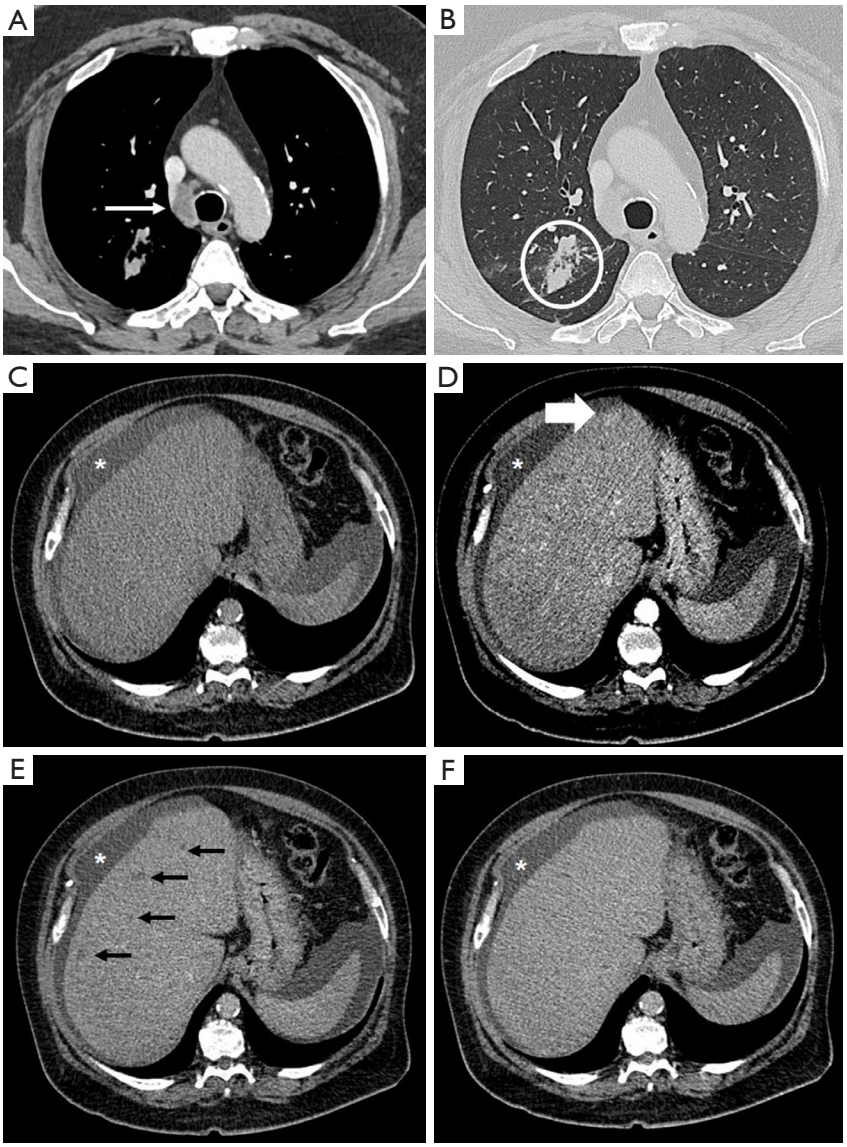

Figure 2 Computed tomography of chest (A,B) and abdomen (C-F). (A,B) Contrast-enhanced scans reveal a parenchymal consolidation suspected of lung cancer in the posterior segment of the right upper lobe (white circle), accompanied by multiple mediastinal lymphadenopathies (thin white arrow). (C) Unenhanced abdominal scan reveals ascites in perihepatic and perisplenic regions (white asterisks), a heterogeneous liver parenchyma with surface nodularity and hypertrophy of the left lobe. (D-F) Contrast-enhanced scans respectively in arterial, portal, and delayed phases confirm multiple tiny hypodense nodules (thin black arrows) and the presence of ascites (white asterisks). Note a hypervascular liver area (D, thick white arrow) without definitive washout in the portal and delayed phases referable to transient hepatic attenuation differences.

cells showing granular and eosinophilic cytoplasm, hyperchromatic nuclei, and unequivocal expression of neuroendocrine markers (such as synaptophysin, chromogranin, CD56 and INSM1). The proliferative index, assessed using Ki-67, was approximately 80% (*Figure 4*). Neither fibrosis nor regeneration nodules were detected in the liver biopsy specimens.

Although no histological examination of right pulmonary consolidation was performed, the patient was discharged with the clinical-radiological diagnosis of metastatic SCLC and the indication to start palliative care in relation to the advanced state of the disease.

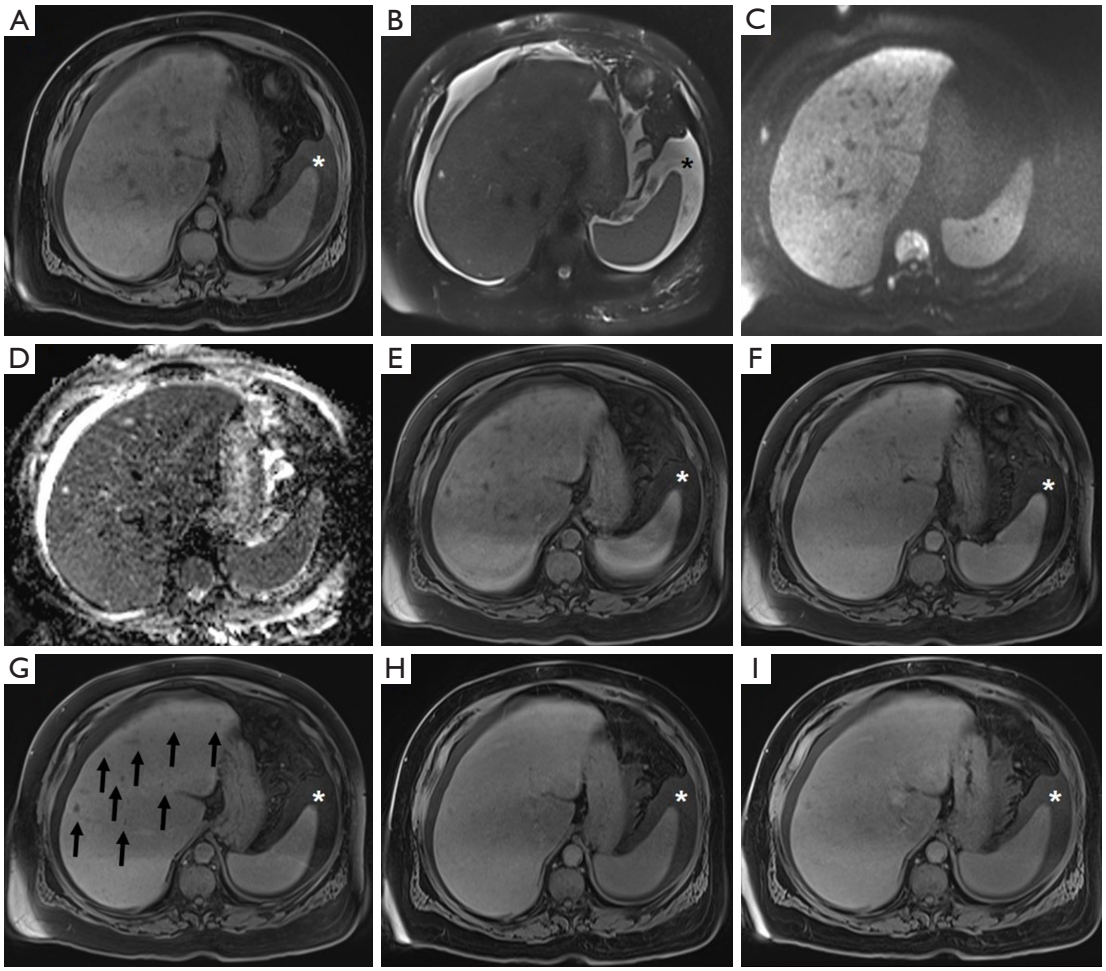

Figure 3 Gd-EOB-DTPA-enhanced magnetic resonance imaging examination of the liver at 1.5 Tesla. (A) Unenhanced T1-weighted VIBE with fat suppression. (B) T2-weighted half-Fourier single-shot turbo spin-echo with fat suppression. (C,D) Echo planar DWI with apparent diffusion coefficient map. (E-I) Contrast-enhanced T1-weighted VIBE with fat suppression respectively in arterial phase, portal phase, delayed phase, 20 minutes, and 35 minutes after contrast agent administration. The examination reveals several liver nodules, best seen in the delayed phase (G, thin black arrows), without arterial phase hyperenhancement or non-peripheral washout. The key sequence is DWI that show a widespread hepatic restriction of proton diffusivity with a signal intensity similar to the spleen (C,D). Note that the hepatobiliary phase of the study cannot be evaluated due to the lack of Gd-EOB-DTPA uptake by the hepatic cells secondary to liver function impairment (H,I) and the presence of ascites (asterisks). VIBE, volumetric interpolated breath-hold examination; DWI, diffusion-weighted imaging; Gd-EOB-DTPA, gadolinium ethoxybenzyl-diethylenetriamine pentaacetic acid.

Discussion

The occurrence of ALF caused by malignant infiltration is uncommon and poses challenges in terms of diagnosis, demanding a heightened level of suspicion, particularly when there is no previous record of primary malignant disease.

Several factors have been implicated in the etiopathogenesis of ALF secondary to miliary liver metastases: extensive infiltration of liver tissue resulting in a significant loss of functional liver mass; infiltration of small bile ducts, leading to severe cholangitis and necrosis; infiltration of hepatic veins, causing ischemic liver damage; sudden ischemia resulting from massive infiltration of malignant cells into sinusoids, leading to hepatocellular necrosis; and cytokine-induced injury, leading to destruction of interlobular bile ducts and portal fibrosis, ultimately resulting in the vanishing bile duct syndrome (7).

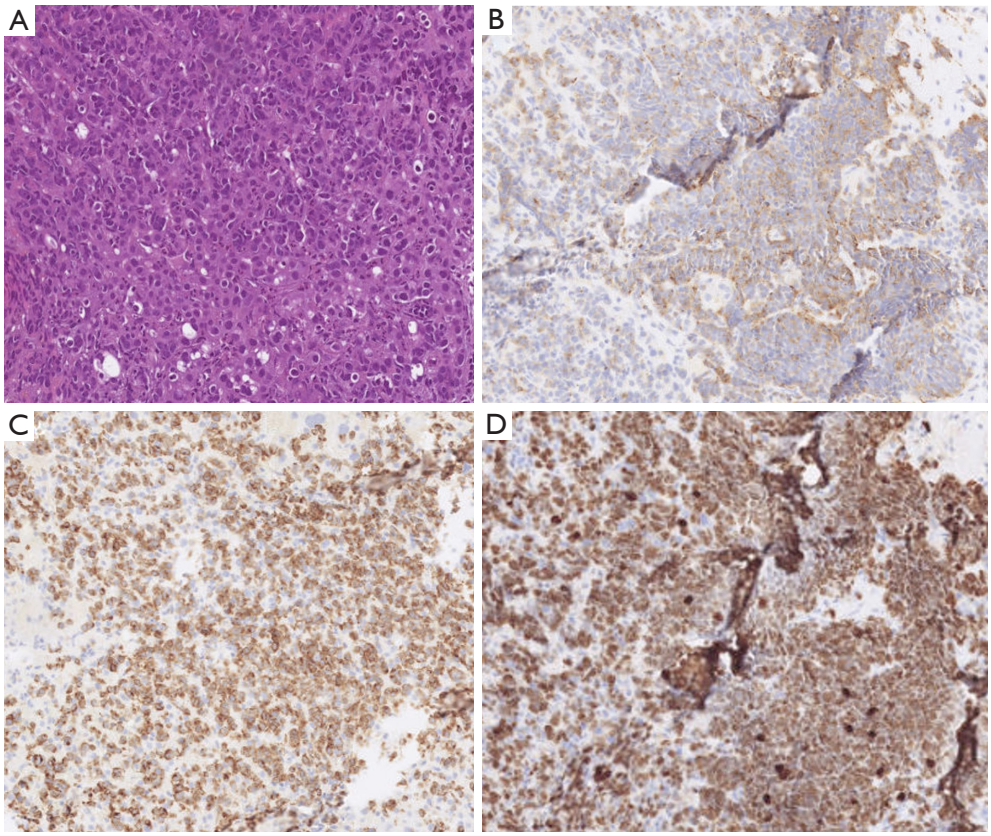

Figure 4 Microscopic and immunostaining findings of liver biopsy. (A) Hematoxylin and eosin stain (magnification, ×40). (B) Chromogranin (magnification, ×40). (C) Synaptophysin (magnification, ×40). (D) Ki-67 (magnification, ×40). The anatomo-pathological analysis shows a tumor characterized by cords and organoid nests of uniform, intermediate-sized, round cells with finely granular and eosinophilic cytoplasm (A). The neuroendocrine carcinoma is positive for chromogranin (B) and synaptophysin (C), and the Ki-67 labeling index is approximately 80% (D).

The clinical picture is nonspecific and dominated by the ALF condition, with common initial signs and symptoms including jaundice, hepatic encephalopathy, and hepatomegaly (3). Routine laboratory test results were generally not effective in detecting the presence of malignancy, except for patients with leukemia. They typically show a hepatocellular pattern of liver injury or an obstructive pattern of liver injury with an increase in AST, ALT, alkaline phosphatase, total bilirubin, and INR values (as in our case) (3).

Imaging plays a crucial role for differential diagnosis in patients with hepatic disease (13,14) but it can lead to erroneous conclusions if not correctly interpreted. Indeed, radiological examinations of patients with malignant liver infiltration often reveal a lack of prominent mass lesions and the disease can be completely undetected (6). Instead, they may display morphological alterations including capsular retraction, reduced hepatic volume accompanied by caudate lobe enlargement, and the presence of liver nodules without the typical major features of hepatocellular carcinoma as described in the Liver Imaging-Reporting & Data System (15). This particular condition has been termed "pseudocirrhosis" due to its resemblance to cirrhotic changes (12). In addition to miliary hepatic metastasis, numerous other conditions can manifest with the radiological picture of "pseudocirrhosis", including sarcoidosis, schistosomiasis, congenital hepatic fibrosis, idiopathic portal hypertension, early primary biliary cirrhosis, chronic Budd-Chiari syndrome, chronic portal vein thrombosis, and nodular regenerative hyperplasia (16). A thorough radiologic examination and careful consideration of clinical factors may be necessary to avoid an incorrect diagnosis, which could potentially have negative consequences for treatment decisions, and

histologic correlation will be essential for diagnosing certain diseases (16). In addition, although NET are frequently associated with hypervascular liver metastases (17), this imaging feature is lost when NET cause malignant hepatic infiltration, as demonstrated in our case.

In our patient, the radiological findings that leaned more toward the diagnosis of liver metastasis than cirrhosis were the presence of a suspected primary pulmonary lesion with associated mediastinal lymphadenopathy and bone lesions, the absence of signs of portal hypertension and hypervascular lesions with typical features of hepatocellular carcinoma, and the widespread liver restriction of proton diffusivity in MRI diffusion-weighted images. Our case highlights also the concept that in patients with severe liver function impairment, the use of Gd-EOB-DTPA as MRI hepatobiliary contrast agent does not help in the detection of diffuse malignant infiltration, even after acquiring images well beyond 20 minutes (the typical delay time of hepatobiliary phase) after intravenous administration (18).

Nuclear medicine techniques can serve as a supplementary tool for imaging of NET when hepatic infiltrative disease is not easily detectable through conventional anatomical imaging methods. Notably, these types of tumors commonly express the somatostatin receptor, making them susceptible to molecular agents that can be used for both imaging and therapeutic purposes (4).

ALF caused by malignancy generally carries a grim prognosis, often leading to death within a span of 2 to 3 weeks (7). Treating ALF resulting from miliary metastasis is often challenging due to the limitations of performing curative surgery and initiating chemotherapy in the presence of liver dysfunction (7,10). The best opportunity for recovery in such patients lies in obtaining an accurate histological diagnosis through liver biopsy and promptly initiating targeted therapy (10).

Conclusions

ALF secondary to malignant liver infiltration represents a rare and challenging scenario that can radiologically mimic cirrhosis and lead to a delayed diagnosis. Imaging, particularly DWI, provides fundamental assistance in reaching an accurate diagnosis, although a biopsy confirmation will still be necessary.

Acknowledgments

Funding: None.

Footnote

Conflicts of Interest: All authors have completed the ICMJE uniform disclosure form (available at https://qims.amegroups.com/article/view/10.21037/qims-23-1037/coif). C.A.M. serves as an unpaid editorial board member of *Quantitative Imaging in Medicine and Surgery*. The other authors have no conflicts of interest.

Ethical Statement: The authors are accountable for all aspects of the work in ensuring that questions related to the accuracy or integrity of any part of the work are appropriately investigated and resolved. All procedures performed in this study were in accordance with the ethical standards of the institutional and/or national research committee(s) and with the Helsinki Declaration (as revised in 2013). Written informed consent was obtained from the patient for publication of this case report and accompanying images. A copy of the written consent is available for review by the editorial office of this journal.

References

1. Vasques F, Cavazza A, Bernal W. Acute liver failure. Curr Opin Crit Care 2022;28:198-207.
2. Rowbotham D, Wendon J, Williams R. Acute liver failure secondary to hepatic infiltration: a single centre experience of 18 cases. Gut 1998;42:576-80.
3. Rich NE, Sanders C, Hughes RS, Fontana RJ, Stravitz RT, Fix O, Han SH, Naugler WE, Zaman A, Lee WM. Malignant infiltration of the liver presenting as acute liver failure. Clin Gastroenterol Hepatol 2015;13:1025-8.
4. D'Souza JC, O'Brien SR, Yang Z, El Jack AK, Pantel AR. Widespread micronodular hepatic metastases of neuroendocrine tumor detected by [68Ga]DOTATATE PET/CT. Radiol Case Rep 2022;18:481-5.
5. Ke E, Gomez JD, Tang K, Sriram KB. Metastatic small-cell lung cancer presenting as fulminant hepatic failure.

BMJ Case Rep 2013;2013:bcr2012007865.
6. Fazio N, Di Meglio G, Lorizzo K, de Brand F. Miliary hepatic metastases from neuroendocrine carcinoma. Dig Surg 2008;25:330.
7. Lavender CA, Stout J, Chung HY, Johnson M, Thandassery RB. Acute Liver Failure due to Miliary Liver Metastasis. ACG Case Rep J 2020;7:e00294.
8. Mishima S, Nozaki Y, Mikami S, Kihira E, Iikura M, Koketsu R, et al. Diffuse Liver Metastasis of Small-Cell Lung Cancer Presenting as Acute Liver Failure and Diagnosed by Transjugular Liver Biopsy: A Rare Case in Whom Nodular Lesions Were Detected by Enhanced CT Examination. Case Rep Gastroenterol 2015;9:81-7.
9. Veloso N, Amaro P, Ferreira M, Romãozinho JM, Sofia C. Acute liver failure secondary to hepatic infiltration by poorly differentiated neuroendocrine tumor. Gastroenterol Hepatol 2014;37:356-7.
10. Yan P, Liu Y, Wang Q, Chen X. A Rare Case of Acute Liver Failure Secondary to Diffuse Hepatic Infiltration of Small Cell Neuroendocrine Carcinoma. Front Oncol 2021;11:616337.
11. Xia Y, Zhang L, Wu H, Qiao L, Xia L. Primary hepatic neuroendocrine tumor with multiple liver metastases: A case report with literature review. J Int Med Res 2020;48:300060520932114.
12. Villani R, Di Cosimo F, Sangineto M, Romano AD, Serviddio G. Pseudocirrhosis and portal hypertension in patients with metastatic cancers: a systematic review and meta-analysis. Sci Rep 2022;12:19865.
13. Wáng YXJ, Wang X, Wu P, Wang Y, Chen W, Chen H, Li J. Topics on quantitative liver magnetic resonance imaging. Quant Imaging Med Surg 2019;9:1840-90.
14. Parillo M, Bernetti C, Altomare C, Beomonte Zobel B, Quattrocchi CC. Extrahepatic abscess and dropped gallstones: a case report and a narrative review of an unusual delayed complication of laparoscopic cholecystectomy. Acta Chir Belg 2023. doi: 10.1080/00015458.2022.2163957.
15. Parillo M, Van der Molen AJ, Asbach P, Elsholtz FHJ, Laghi A, Ronot M, Wu JS, Mallio CA, Quattrocchi CC. The role of iodinated contrast media in computed tomography structured Reporting and Data Systems (RADS): a narrative review. Quant Imaging Med Surg 2023. doi: 10.21037/qims-23-603
16. Jha P, Poder L, Wang ZJ, Westphalen AC, Yeh BM, Coakley FV. Radiologic mimics of cirrhosis. AJR Am J Roentgenol 2010;194:993-9.
17. Ozaki K, Higuchi S, Kimura H, Gabata T. Liver Metastases: Correlation between Imaging Features and Pathomolecular Environments. Radiographics 2022;42:1994-2013.
18. Wang C, Yuan XD, Wu N, Sun WR, Tian Y. Optimization of hepatobiliary phase imaging in gadoxetic acid-enhanced magnetic resonance imaging: a narrative review. Quant Imaging Med Surg 2023;13:1972-82.

Cite this article as: Parillo M, Vaccarino F, Taffon C, Vantaggi S, Rossi SM, Beomonte Zobel B, Mallio CA. Imaging findings in malignant hepatic infiltration from neuroendocrine tumor presenting with acute liver failure and mimicking cirrhosis: a case description. Quant Imaging Med Surg 2024;14(1):1193-1199. doi: 10.21037/qims-23-1037

